NECK LOCALIZATION AND GEOMETRY QUANTIFICATION OF INTRACRANIAL ANEURYSMS

E. Sgouritsa[a], A. Mohamed[b], H. Morsi[c,d], H. Shaltoni[d], M. E. Mawad[c,d], I. A. Kakadiaris[a]

[a]Computational Biomedicine Lab, Dept. of Computer Science, University of Houston, Houston, TX
[b]Siemens Corporate Research, Inc., Princeton, NJ; [c]Baylor College of Medicine, Houston, TX
[d]St Luke's Episcopal Hospital, Houston, TX

ABSTRACT

We present an approach for accurate localization of the neck of intracranial aneurysms and quantification of their geometry that is useful for their treatment through endovascular embolization. In particular, we first obtain a vessel segmentation using a topology-preserving level set method and extract the surface of the segmented vessel. We then separate the aneurysm from the parent vessels and localize its neck by formulating the aneurysm segmentation problem as an s-t minimum cut problem. Finally, we estimate clinically relevant geometric parameters of the aneurysm. The results indicate that there is good agreement between the measurements obtained by the proposed approach and two independent manual sets of measurements obtained by two experienced interventional neuroradiologists.

Index Terms— Angiography, neck localization, endovascular embolization, intracranial aneurysm

1. INTRODUCTION

An aneurysm is a focal disease of the wall of an artery, leading to its bulging or dilatation. Intracranial aneurysms bear the risk of rupture, which may lead to mortality. Through the use of stents, wire coils, and other embolic material or devices, the endovascular treatment of aneurysms aims at creating a thrombus inside the aneurysm, thereby preventing its growth and reducing its risk of rupture. The selection and use of these devices requires accurate examination and quantification of the geometry of the aneurysm and its parent arteries. Most of the related approaches separate an intracranial aneurysm from the neighboring vasculature, but do not attempt to extract measurements that are necessary for treatment planning [1]. In this paper, we improve our previous work [2] on neck localization and extraction of patient-specific geometric parameters [3] of intracranial saccular aneurysms, based on 3D angiographic images, presenting a more stable and accurate approach. The main contributions of this work are: i) an accurate and topologically correct vasculature segmentation method using topology-preserving level sets and ii) an aneurysm segmentation and neck localization method using graph-cuts which guarantees a globally optimal solution.

This work was supported in part by Siemens Medical Solutions, USA and the UH Eckhard Pfeiffer Endowment Fund. The authors would like to thank Dr. Andrew F. Hall and Dr. Klaus Klingenbeck-Regn for their support. Any opinions, findings, conclusions or recommendations expressed in this material are of the authors and may not reflect the views of the sponsors.

2. METHODS

Our approach first segments the vessel using a topology-preserving level set method as described in Section 2.1. Based on the 3D mesh surface extracted from the vessel segmentation, a graph is created. Next, an s-t graph-cut approach is employed to accurately segment the aneurysm and localize its neck (Section 2.2). Finally, clinically relevant geometric parameters are estimated as presented in Section 2.3.

2.1. Vessel Segmentation

A topologically correct vessel segmentation is necessary for constructing accurate geometric models for shape and geometry quantification of the aneurysm and computational fluid dynamics simulations. Thus, we employ a topology-preserving level set method similar to that presented by Han *et al.* [4] to segment the vessel. This method guarantees that, throughout the level set evolution process, the topology of the implicit curves or surfaces is preserved.

We first crop the 3D volume to a region of interest including the aneurysm and the surrounding vasculature. Since the anatomy of the vessel is known *a priori* (i.e., it does not contain any holes or handles), the level set is initialized as a sphere inside the vessel. During the evolution, the topology of the sphere is preserved, therefore the final vessel segmentation result can be guaranteed to be topologically equivalent to a sphere. We choose the evolution equation defined by Chan and Vese [5], as it can handle noisy images and can detect objects whose boundaries are not always preserved or necessarily defined by gradient. Figure 1 illustrates the difference between the segmentation of a specific vessel using a

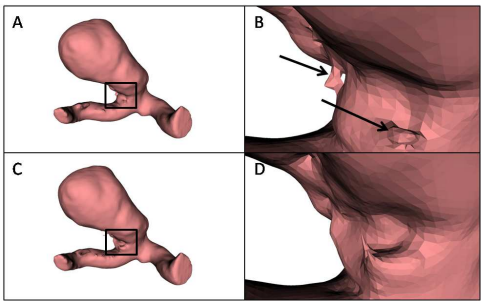

Fig. 1. (A) Vessel segmentation result using a thresholding approach. (B) Depiction of the boxed region in (A) in higher detail - arrows indicate handles in the generated surface. (C) Vessel segmentation result using topology-preserving level sets. (D) Depiction of the boxed region in (C) in higher detail - the generated surface is topologically correct.

thresholding approach [6] (Figs. 1(A, B)) and the topology-preserving approach (Figs. 1(C, D)) described above. The thresholding approach generates handles on the surface of the vessel, whereas the topology-preserving approach creates a single genus zero surface.

2.2. Aneurysm Segmentation and Neck Localization

The goal of this step is to separate the vessel surface, extracted from the segmented vessel, into two components: the aneurysm and the parent arteries, and to localize the neck of the aneurysm. For that, we adopt a graph-based approach.

Let $G = (V, E)$ be a graph with vertices V and edges E, where every edge is assigned a non-negative cost. The set V includes two vertices called terminals, namely the source, S, and the sink, T. A subset of edges $C \subset E$ is called an s-t cut if the terminal vertices in the induced graph $\mathbb{G} = (V, E - C)$ are completely separated (i.e., there is no path from source to sink). The cost of the cut is the sum of the weights of all the edges in C. The problem of finding the cut with the smallest cost is referred to as the s-t min-cut problem and it can be solved in polynomial time [7].

To segment the aneurysm from the neighboring vessels, we follow an approach inspired by the work of Boykov *et al.* [8]. A graph is created consisting of the vertices P of the mesh of the vessel surface and the two terminal nodes. Therefore, $V = P \cup \{S, T\}$. The graph consists of two types of undirected edges: the n-links and the t-links. The n-links consist of all the edges M of the vessel mesh. The t-links consist of connections between vertices of the mesh and terminals.

In particular, the source vertex is connected to a set of vertices, A, which is known *a priori* to belong to the aneurysm (Fig. 2(A)). To identify those vertices, the centerlines of the parent vessels to which the aneurysm is attached need to be

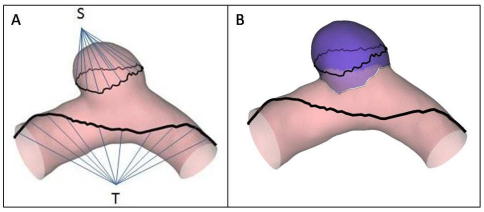

Fig. 2. (A) Illustration of the s-t graph used for aneurysm segmentation. (B) Aneurysm segmentation result depicting the aneurysm (purple) and the neck contour (white).

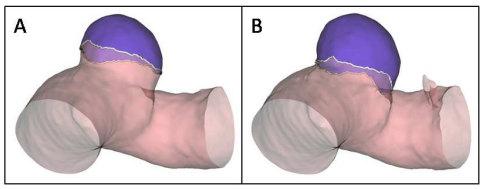

Fig. 3. Aneurysm segmentation result obtained using an active contour model (A) and graph-cuts (B).

determined first. The centerlines are determined as the paths on the Voronoi diagram of the vessel surface that minimize the integral of the radius of the maximal inscribed spheres along the path [9]. The user is required to provide only one end-point per branch. All parts of the vessel surface that are farther than a local vessel width-dependant distance from the centerlines of the parent vessels are extracted. The vertices lying on the boundary between the largest connected component of those parts and the rest of the vessel mesh define the set A. The sink vertex is connected to a set of vertices B which is known *a priori* to belong to the parent vessels (Fig. 2(A)). The set B consists of the vertices lying on the shortest geodesic paths between the vertices on the vessel surface that are the closest to the user-provided end-points. Therefore, $E = M \underset{p \in A}{\cup} \{S, p\} \underset{q \in B}{\cup} \{q, T\}$.

Assuming that the neck of the aneurysm is characterized by high curvature of the vessel surface, we assign appropriate costs to the edges of the graph such that the minimum cut consists of edges of high curvature, around the neck. Particularly, concerning the n-links, we assign a cost to each edge $\{p, q\} \in M$ equal to $\exp\left(0.5 * \left(curv\left(p\right) + curv\left(q\right)\right)\right)$, where $curv\left(i\right)$ is the Gaussian curvature of the mesh at the vertex $i \in P$. Additionally, we assign a very high cost to all the t-links, which imposes hard constraints on the vertices that are known *a priori* to belong either to the aneurysm or to the parent vessels. The weights of the edges are summarized in Table 1. The minimum cut of the constructed graph defines the aneurysm segmentation and the localization of its neck (Fig. 2(B)).

In our previous approach [2], an active contour model was used to localize the neck of the aneurysm. The main limita-

Table 1. Edge weights of the graph

Edge	Weight	For
$\{p,q\}$	$\exp\{0.5 * [curv\,(p) + curv\,(q)]\}$	$\{p,q\} \in M$
$\{S,p\}$	∞	$p \in A$
$\{p,T\}$	∞	$p \in B$

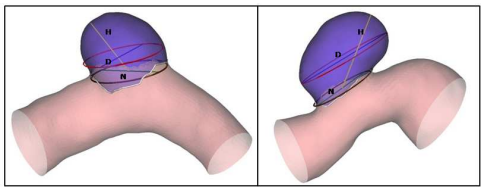

Fig. 4. Depiction of the (i) fitted ellipse of the aneurysm neck (brown) and maximum diameter (red), (ii) lines marking the estimated N (green), H (yellow), and D (blue).

tions of that approach were that the contour stopped evolving after reaching a local minimum (Fig. 3(A)) and the fact that self-intersections had to be resolved after each iteration. The graph-cuts based method as described above guarantees a globally optimal solution while restricting the set of feasible solutions for the neck to single closed contours (Fig. 3(B)), thus, eliminating the limitations of our previous work.

2.3. Aneurysm Geometry Quantification

This step aims at estimating geometric parameters of the aneurysm surface extracted from the previous step. We compute the following measurements: neck length (N), dome height (H) and maximum diameter (D) as described by Mohamed *et al.* [2]. Figure 4 illustrates their location in the case of two saccular ("berry shaped") aneurysms.

3. RESULTS AND DISCUSSION

The proposed approach is implemented using the Insight Segmentation Toolkit (ITK), the Visualization Toolkit (VTK), and the Vascular Modeling Toolkit (VMTK). We report results on 19 three-dimensional (3D) Digital Subtraction Angiography (DSA) datasets (*syngo* Inspace 3D, Siemens AG, Forchheim, Germany) of saccular aneurysms. All image slices are 512×512 pixels in size, with isotropic voxels of, typically, 0.4 mm in size, and the number of slices per dataset varies from 187 to 481. The database contains data of aneurysms arising from 14 internal carotid arteries (ICA), 4 anterior communicating arteries (AComm) and 1 basilar tip.

Manual measurements of N, H, and D of aneurysms in the database were obtained independently by two experienced interventional neuroradiologists (readers R_1 and R_2) through the conventional treatment planning approach. Table 2 includes the average difference (Bias) and the standard deviation of the difference (STD) between the readers' measurements (first row) and between the proposed method ($CAPETA$ 2) and each of the readers (second and third rows). For the purposes of this work, three different cohorts are employed: the first cohort (C_1) contains all 19 datasets, while the second (C_2) and third (C_3) cohorts contain 17 datasets (each a different subset of C_1). Excluded datasets' measurements considerably deviated from the readers' measurements mainly due to inaccurate vessel segmentation as a result of close proximity of the aneurysm to its parent vessels. Results are reported for N, H, and D from C_1 (first three columns of Table 2) and for N (fourth column of Table 2) and H (fifth column of Table 2) obtained from C_2 and C_3, respectively. The Bland-Altman plots for N from the C_2 cohort are presented in Fig. 5.

We can observe (see Table 2) that the proposed method provides accurate estimates of the maximum diameter obtained from the C_1 cohort. The STDs of the differences between the D measurements obtained by our approach and each of the readers are 0.87 mm and 2.02 mm, respectively, while the STD of the difference between the readers is 1.76 mm. Results for N and H from the C_2 and C_3 cohorts, respectively, are improved compared to those from C_1. The STDs of the differences between our measurements and each of the readers for N and H are reduced becoming similar to that between the readers (0.73 mm and 0.64 mm, respectively). It should to be noted that the constant bias ($\approx$ 1 mm) for the neck length measurement is related to the method used to acquire the manual measurements. The readers measure relevant geometric parameters based on volume rendered images generated through a user-controlled transfer function. This rendering approach effectively produces a visualization of thresholded segmented blood vessels. This segmentation is different from the one produced through our approach, a fact that can create discrepancies between the two measurements. Specifically, for a dataset for which our measurement for the neck length is 5.34 mm, the expert's measurement is 4.1 mm when using his vessel segmentation and 5.19 mm when using ours. Some discrepancies can also be attributed to the convention used for the neck measurement. Our approach computes the neck as the major axis of the ellipse approximating the neck contour [2], whereas the experts measure it on the 2D projection of the dataset along the length of the parent artery.

Concerning the vessel segmentation step, the result can depend heavily on the initialization of the level set function. The vessel segmentation is always topologically correct but the topology can be preserved in different ways. As a result, the segmentation does not always reflect the anatomy of the vessel (Fig. 6), a fact that can affect the next stage of the algorithm. For example, the dataset illustrated in Fig. 6(B) was excluded from C_3 because the inaccurate segmentation, as a

Table 2. Average difference (Bias) and standard deviation of the difference (STD) between the measurements of the readers (R_1 and R_2) and the proposed method ($CAPETA$ 2) for N, H and D using C_1, C_2 and C_3 cohorts.

	N (C_1) (mm)		H (C_1) (mm)		D (C_1) (mm)		N (C_2) (mm)		H (C_3) (mm)	
	Bias	STD	Bias	STD	Bias	STD	Bias	STD	Bias	STD
R_1 vs. R_2	0.03	0.70	0.49	0.65	-0.74	1.76	0.05	**0.73**	0.41	**0.64**
$CAPETA$ 2 vs. R_1	1.12	1.18	0.44	1.40	0.72	0.87	0.84	**0.74**	0.04	**0.63**
$CAPETA$ 2 vs. R_2	1.15	1.12	0.93	1.59	-0.01	2.02	0.89	**0.63**	0.44	**0.52**

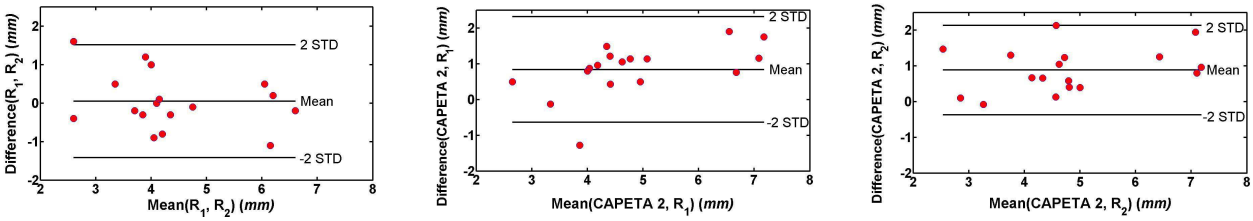

Fig. 5. Bland-Altman plots for the analysis of the difference between the neck length (N) measurements of the two expert readers (R_1 and R_2) and the proposed approach ($CAPETA$ 2) when using the C_2 cohort (17 datasets).

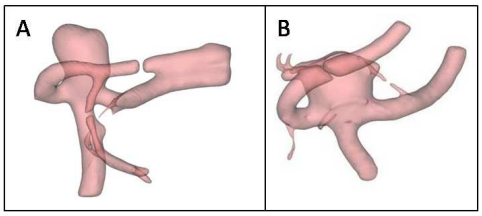

Fig. 6. Vessel segmentation result for two datasets for which, although the surface of the segmented vessel is topologically correct, the segmentation does not reflect the anatomy of the vessel (touching vessels).

result of close proximity of the aneurysm to the parent vessel, caused an overestimation of the H measurement.

4. CONCLUSION

We presented an approach for neck localization and quantification of geometric parameters of intracranial aneurysms. The results indicate that there is good agreement between the measurements obtained by the proposed approach and the manual measurements obtained by two experienced interventional neuroradiologists. The presented method performs better when compared to our previous work [2], since it guarantees a topologically correct vessel segmentation and provides a global solution for the localization of the neck.

5. REFERENCES

[1] W.C.K. Wong and A.C.S. Chung, "Augmented vessels for quantitative analysis of vascular abnormalities and endovascular treatment planning," *IEEE Transactions on Medical Imaging*, vol. 25, no. 6, pp. 665–684, 2006.

[2] A. Mohamed, E. Sgouritsa, H. Morsi, H. Shaltoni, M.E. Mawad, and I.A. Kakadiaris, "Computer-aided planning for endovascular treatment of intracranial aneurysms," in *Proc. Society of Photographic Instrumentation Engineers Medical Imaging Conference*, San Diego, CA, Feb. 13-18 2010 (In Press).

[3] L. Parlea, R. Fahrig, D.W. Holdsworth, and S.P. Lownie, "An analysis of the geometry of saccular intracranial aneurysms," *American Journal of Neuroradiology*, vol. 20, no. 6, pp. 1079–1089, 1999.

[4] X. Han, C. Xu, and J.L. Prince, "A topology preserving level set method for geometric deformable models," *IEEE Transactions on Pattern Analysis and Machine Intelligence*, vol. 25, no. 6, pp. 755–768, 2003.

[5] T.F. Chan and L.A. Vese, "Active contours without edges," *IEEE Transactions on Image Processing*, vol. 10, no. 2, pp. 266–277, Feb. 2001.

[6] N. Otsu, "A threshold selection method from gray-level histograms," *Automatica*, vol. 11, pp. 285–296, 1975.

[7] L. Ford and D. Fulkerson, *Flows in networks*, Princeton University Press, 1962.

[8] Y. Boykov and G. Funka-Lea, "Graph cuts and efficient N-D image segmentation," *International Journal of Computer Vision*, vol. 70, no. 2, pp. 109–131, 2006.

[9] L. Antiga and D. A. Steinman, "Vascular modeling toolkit," Available-Online: http://www.vmtk.org, Jan. 26 2009.